Exploring the potential of di-boron di-nitride monolayer (o-B2N2) as a K-ion battery anode: A DFT study

Ali A. Rajhi [a], Eduardo Hernández [b,*], Carlos Serrano [b], Shelesh Krishna Saraswat [c,**], Ahmed Mohammed Mahmood [d], Hayder sharif [e], Y.A. Abdulsayed [f], Ahmed Alawadi [g]

[a] *Department of Mechanical Engineering, College of Engineering, King Khalid University, Abha, 61421, Saudi Arabia*
[b] *Facultad de Mecánica, Escuela Superior Politécnica de Chimborazo (ESPOCH), Riobamba, 060155, Ecuador*
[c] *Department of Electronics and Communication GLA University, Mathura, 281406, India*
[d] *Department of Optical Techniques, Al-Noor University College, Nineveh, Iraq*
[e] *Medical Technical College, Al-Farahidi University, Iraq*
[f] *Department of Optical Techniques, Al-Zahrawi University College, Karbala, Iraq*
[g] *College of Technical Engineering, The Islamic University, Najaf, Iraq*

ARTICLE INFO

ABSTRACT

Due to favorable future use of electrochemical energy storage systems in portable electronic devices, these systems have received much attention. Employing these systems in "smart" clothes equipped with piezoelectric pieces to gain energy from body movement and roll-up displays is promising. Nevertheless, further development of these technologies is a significant challenge due to lack of appropriate battery electrodes that supply desirable electrochemical performance. 2D flexible and light materials with remarkable chemical and physical attributes such as acceptable conductivity, high surface metal diffusivity, hydrophilic surfaces, and mechanical strengths were introduced as potential options for battery electrodes. In present research, 2D orthorhombic di-boron di-nitride monolayer (o-B_2N_2) as a novel 2D boron nitride allotrope has been investigated. Systematically, various impacting factors like their electrochemical and electronic features (theoretical capacity, equilibrium voltage, binding strength, etc.) were investigated. It is noteworthy that specific capacity of K-ion batteries (KIBs) reaches 2347 mAh.g^{-1}. In addition, the existence of o-B_2N_2 ring accelerates the diffusion of K-ions, and diffusion barriers are 0.14 eV. Mean open circuit voltage (OCV) and low diffusion barrier of o-B_2N_2 monolayer guarantee long service life and fast charging/discharging for practical purposes. Based on results, monolayer o-B_2N_2 is proper as a high-performance negative electrode material in KIBs.

1. Introduction

From electric vehicles and portable devices to various electronic devices and large power grids, energy storage systems have a great effect on human life in recent years [1–3]. Because of lightweight, long cyclability, and high energy storage efficiency of rechargeable lithium-ion batteries (LIBs), they are market leaders in energy storage [4–7]. Despite its potential for sustainable development and commercialization, this energy storage technology faces some challenges, including limited lithium resources, low safety, and low theoretical specific capacity [8]. Therefore, finding alternate battery systems, particularly non-lithium-ion anode materials that have high energy

storage abilities, is a crucial requirement. Potassium-ion batteries (KIBs) have attracted much attention because potassium ions (K) have similar properties to lithium (Li) since their group is the same in periodic table. Replacing lithium with potassium because of its natural abundance can reduce dependence on lithium sources [9–11]. Moreover, K is softer than lithium and can significantly prevent dendrite formation in LIBs. Meanwhile, KIBs offer an ultra-high rate of charging and discharging [12].

Currently, design of appropriate anode materials for KIBs is a fundamental challenge. Various high performance anode materials that are well developed for LIBs may not be proper for KIBs. Because of larger atomic radius of potassium compared to lithium, K atoms can barely fit

---

into these anode materials [13]. Since atomic radius between graphite layers is large, it is tough to insert K ions between these layers, so graphite, which is commonly employed for embedding Li ions, is not a favorable electrode material for KIBs [14–17]. It is also possible to form 2D heterostructures by combining other 2D layer materials with graphene. Despite tight filling between layers of heterostructure electrodes which restricts ion transport, they possess electrochemical stability, high capacity, and high conductivity [18].

Whereas hexagonal boron nitride (h-BN) is considered most comprehensive studied two-dimensional material because of its considerable potential in nano-electronics due to its indirect broad band gap of 6 eV [19], weak function of this material is also most likely due to its wide band gap, given that negative electrodes require superior electronic conductivity [20], inadequate interaction between hexagonal boron nitride surface and alkali-metals merged with poor lithium adsorption for conversion of its indirect wide band gap to metalized structure, as well as hampering its additional applicability in energy storage purposes [21–24]. Novel two-dimensional polymorph of graphene-like BN with orthorhombic system (o-B2N2) that has been introduced recently by Demirci et al. [25], was anticipated via DFT framework. According to in-depth studies of mechanical and dynamic stability, o-B_2N_2 monolayer has stability from both points of view. A further study indicated that o-B_2N_2 maintained integrity of geometrical structure to 1000 K for 10 ps employing Ab-initio molecular dynamics calculations [26]. Novel o-B_2N_2, which is a semiconductor with a direct narrowing band gap of 0.64 eV, offers various potential applications in storage and conversion of energy, such as hydrogen storage, rechargeable batteries, and photovoltaic [25,27,28]. Most importantly, regarding both N and B are light elements with molecular weights of 14.00 and 10.8 a.u., it is anticipated that o-B_2N_2 can potentially lead to a superior theoretical specific capacity for rechargeable batteries [26].

In present research, applicability of two-dimensional o-B2N2 for KIB electrodes has been investigated systematically for the first time via DFT computations. Investigations were started by electronic features and structural geometry optimization of o-B2N2 monolayer. Thereafter, binding strength of K at feasible appropriate binding sites on o-B2N2 surface was computed employing DFT and DFT-D3. Based on DFT-D3 calculations, theoretical capacity and equilibrium voltage have been studied with a global optimization method. In o-B2N2 monolayer, ionic diffusion during polarization, deformation charge density after single K-atom adsorption, and charge transfer (CT) have been computed. A comprehensive comparison with other 2D materials recently promising for battery applications reveals that novel two-dimensional o-B2N2 monolayers present KIB anode materials with remarkably low ionic mobility and extremely high theoretical specific capacities. It has been shown that it can be introduced as an attractive complementary material.

2. Computational methods

Electronic analysis, geometry optimization, and energy calculations were performed using the B3LYP functionality and the 6-31G (d) base set. Grimme's variance term 'D3′' was used to accurately predict weak interactions [29]. A literature survey shows that B3LYP is a suitable function to calculate the structural and electronic properties of several nanomaterials [30–34]. In present work, GAMESS software has been employed to carry out all of computations [35]. By Bader charge approach, CT between o-B2N2 substrates and K ions has been analyzed [36]. Also, by applying nudged elastic band (NEB) approach, energy of diffusion barrier has been obtained and diffusion paths of K ions have been computed [37,38]. Moreover, adsorption energy (Ead) of K atom on o-B2N2 substrates is obtainable by Ref. [39]:

$$E_{ad} = \frac{\left(E_{K@o-B_2N_2} - \left(E_{o-B_2N_2} + xE_K\right)\right)}{x} + E_{BSSE} \tag{1}$$

According to following half-cell reactions, charge/discharge

processes of o-B_2N_2 monolayer have been simplified:

$$xK^+ + xe^- + o - B_2N_2 \leftrightarrow K_x@o - B_2N_2 \tag{2}$$
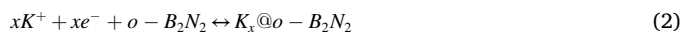
In order to compute open-circuit voltage (VOCV), following equation can be achieved based on aforementioned reaction [39]:

$$VOCV = \frac{\left(E_{K@o-B_2N_2} - \left(E_{o-B_2N_2} + xE_K\right)\right)}{xe} \tag{3}$$

where number of K atoms, energy of a K atom in the bulk system, energy of pristine monolayer, and total energy of K adsorbed on o-B2N2 monolayer are represented by x, E_K, E_{o-B2N2}, and $E_{K@o-B2N2}$, respectively. Adsorption of K metal atom on pristine monolayer is confirmed by negative values of E_{ad}. Maximum storage capacity C can be determined as below [40]:

$$C = \frac{x_{max}F}{M} \tag{4}$$

where Faraday constant, number of adsorbed potassium at maximum adsorption concentration, and atomic mass are represented by F (26.81 A h mol^{-1}), x_{max}, and M, respectively.

3. Results and discussion

3.1. Electronic and structural attributes

Despite significant progress achieved, efforts to identify improved two-dimensional materials and further designs that supply outstanding battery function are at early phases of development. Although electronic conductivity of anode materials has been considered a critical screening aspect in investigation of charging/discharging performance, it has not been well studied so far [41]. In anode materials, favorable conductivity is demanded for electron transfer. In this regard, highly conductive metallic conductors or semiconductors are the most appropriate anode materials. However, as discovery of materials with high-insulation feature as battery electrodes enhances, more focus must be dedicated to this facet via computational and theoretical methods. Because of futuristic applicability of h-BN, which has graphene-like structure, it is the most broadly investigated two-dimensional material with numerous universal applications (Fig. 1a, b) [42]. Nonetheless, its final utilization anode material in rechargeable batteries is restricted by its limited electrochemical attributes and vast band gap [22].

Therefore, a different stable structure for BN has been proposed. This new structure is created by rearranging the positions of nitrogen and boron atoms in a geometrical manner, resulting in a structure that has high electrical conductivity and works well as an electrode in KIBs. Recently reported by Dimiciri et al. [25] via DFT calculation, o-B_2N_2 is a novel two-dimensional material polymorph of BN group, which is similar to graphene and h-BN in its honeycomb crystalline structure. Upside view of completely optimized structure o-B_2N_2 and h-BN monolayers is shown in Fig. 1b the ring of o-B_2N_2 was constructed with 4 atoms, which include alternating nitrogen-nitrogen, boron-nitrogen, and boron-boron bonds. Optimized Bravais vectors of o-B_2N_2 are 4.57 Å 2.46 Å for a and b, respectively, and nitrogen–nitrogen, boron–nitrogen, and boron–boron bond distances are 1.44 Å, 1.44 Å, and 1.73 Å respectively, which match with former investigations [25].

For more comprehension nature of o-B_2N_2 chemical bonds and for characterization the of electron localization in interstitial spaces, valence electron localization function have been calculated, electron distributions are mainly placed in boron–boron, boron–nitrogen, and nitrogen–nitrogen bonds in comparison to hollow areas that electron localization is close to 0. These findings reveal covalent bonding features in o-B_2N_2 surface. Furthermore, the researchers conducted a Bader charge analysis to determine the net charge on the nitrogen and boron atoms, which was found to be approximately +0.92 |e| and −0.92 |e|, respectively. They also calculated the electronic band structure and
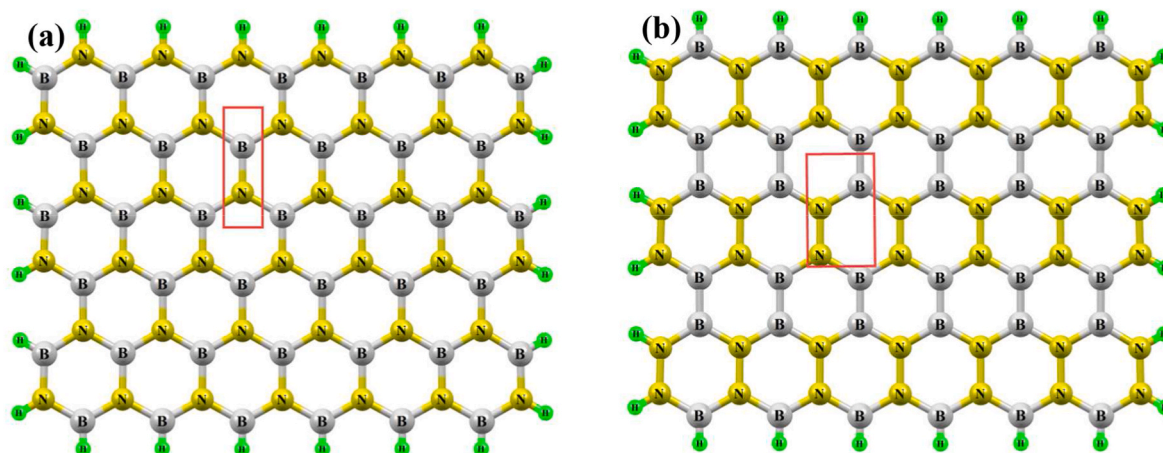
Fig. 1. Top view of a free-standing (a) hexagonal boron nitride and (b) o-B_2N_2 monolayers.

density of states (DOS) for the o-B_2N_2 monolayers based on the optimized structure parameters. Results indicated that o-B_2N_2 is a semiconductor with 0.75 eV electronic band gap (see Figs. 1S and 2S), which is much smaller than hexagonal boron nitride.

3.2. Single K atom adsorption on o-B_2N_2 surface

In most cases, a futuristic anode material for K based batteries needs a relatively considerable binding strength of K as a basic requirement. As a result, we used the DFT-D3 approach to calculate the binding energy between a single potassium atom and different possible binding sites on the o-B_2N_2 structure. During K intercalation, large monolayer with 10*15 Å has been selected to prevent interactions between adjacent K-ions on surface of o-B_2N_2. Because of D_{2h} symmetry of o-B_2N_2 monolayer, 7 potential binding units have been supposed at start of calculations, which can be classified in three types represented by T (top), B (Bridge), H (hollow) as indicated in Fig. 2a. First group includes H1 and H2 placed top of hollow site for B_4N_2- and B_2N_4-Hexagon, respectively. Second one includes TN and TB locating above any nitrogen- and boron-atom based on crystal symmetry. Also, third type has B1, B2, B3 that locate between boron–boron and nitrogen–nitrogen, boron–nitrogen bonds, respectively.

A negative binding strength suggests a more stable binding configuration, which reveals scattering rather than clustering of adsorbed K-atoms. Hence, during charging/discharging process, formation of metal-

clusters or metal-dendrites should be considered and prevented. In studied binding areas, H1 and H2 indicate lowest binding strength for K atom and residual adsorption areas have shifted to H1 or H2 sites. For two most stable binding sites, work function, CT, binding height, and calculated binding strength are listed in Table 1. H1 exhibits a binding strength for K atoms of −0.398 eV, which is the lowest of all the atoms (Full geometry optimization of K atom at H1 is shown in Fig. 2b). In comparison to recently reported two-dimensional materials, these binding strengths are considerably large [43]. The binding energy for other sites was provided in Table 1. This indicates a faster charge procedure with a wider binding interaction happening between K atom and orthorhombic B_2N_2 against weak binding to metal ions in h-BN monolayer [21]. More important, a uniform distribution of K atoms on surface

Table 1
E_{ad} employing density functional theory and DFT-D3, binding height, CT, and barrier energy of adsorbed K over the most desirable binding sites.

Site	$E_{ad\text{-}DFT}$ (eV)	$E_{ad\text{-}DFT\text{-}D3}$ (eV)	Q (e)	E_b (eV)
H1	−0.397	−0.478	0.889	0.14
H2	−0.143	−0.254	0.653	0.29
B1	−0.083	−0.115	0.237	–
B2	−0.057	−0.090	0.165	–
T1	0.120	0.102	0.088	–
T2	0.167	0.134	0.821	–

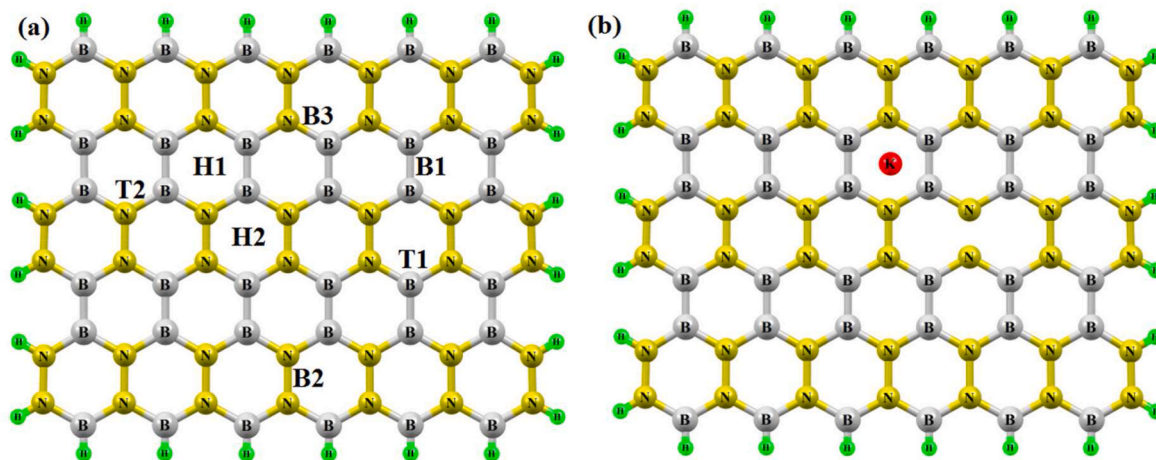**Fig. 2.** (a) Appropriate binding sites for K on free-standing o-B_2N_2 monolayer (T2/T1 represent binding sites above of nitrogen/boron atoms; H1 and H2 refer to hollow-sites of hexagonal B_4N_2-ring and B_2N_4-ring, respectively; binding sites at boron–boron, nitrogen–nitrogen, and boron–nitrogen bridges are represented by B1, B2, and B3, respectively). (b) Upside vision of the most stable optimized configuration of single adsorbed K atom on o-B_2N_2 monolayer.

of o-B_2N_2 via intercalation mechanism instead of accumulating for metal-dendrites formation is indicated by results. These findings guarantee safety, stability, and better reversibility of KIBs. In addition, after K adsorption on the o-B_2N_2 sheet, this surface showed metallic behavior based on DOS analysis as shown in Fig. 3S.

3.3. Average OCV and theoretical storage capacity

By step-wise inserting K-ion over both sides of o-B_2N_2 surface, OCV and high-record theoretical specific capacity of this monolayer have been studied. As we know, H1 and H2 had more energetic stability among all binding areas. First, K atoms are evenly inserted into H1 on both sides of the o-B_2N_2 surface to form the first K layer until it is fully restored. Subsequently, K atoms were localized to H2 by formation of a second K layer, and a series of intermediates between $K_x@B_2N_2$ (x = 0.5, 1.0, 1.5, 2.0, 2.5, 3, 0) were considered (Fig. 4S). Dendrite formation is prevented by keeping all binding energies of all configurations negative via charging mechanism. Therefore, o-B_2N_2 can store a maximum of $K_2@B_2N_2$ for KIBs. Based on these results, o-B_2N_2 anode material has a theoretical specific K storage capacity of approximately 2347 mAh g^{-1}. Moreover, it is valuable to highlight extraordinary K storage capacity in this new monolayer. It can be clearly seen that this material has a considerably larger K storage capacity than other two-dimensional materials [44–47].

Potential voltage is another factor in assessing high efficiency of KIBs. OCV is indicated by dark line in Fig. 3, which is a function of K concentration. All average OCVs are positive, affirming applicability of o-B_2N_2 monolayer as anode for KIBs. Furthermore, by increasing the K ion concentration, the OCV shows a decreasing trend across the three (K) insertion potential plateaus, with an average voltage of ~0.292 V. With average voltages, maximum power density can be achieved via the charging/discharging processes, and K-dendrites can be effectively prevented, improving electrode stability. Therefore, o-B_2N_2 monolayer can be employed as a high-performance negative electrode for KIBs.

3.4. Diffusion kinetics and charge transfer

Improvement of high-performance KIBs crucially relies on ability of anode materials particularly charging/discharging processes, which are generally driven by kinetic attributes of CT. Therefore, we investigated the charge density differences of the adsorbed K atoms at the most desirable sites on the o-B_2N_2 monolayer. For both systems, charge accumulation and depletion are indicated in Fig. 4 as three-dimensional
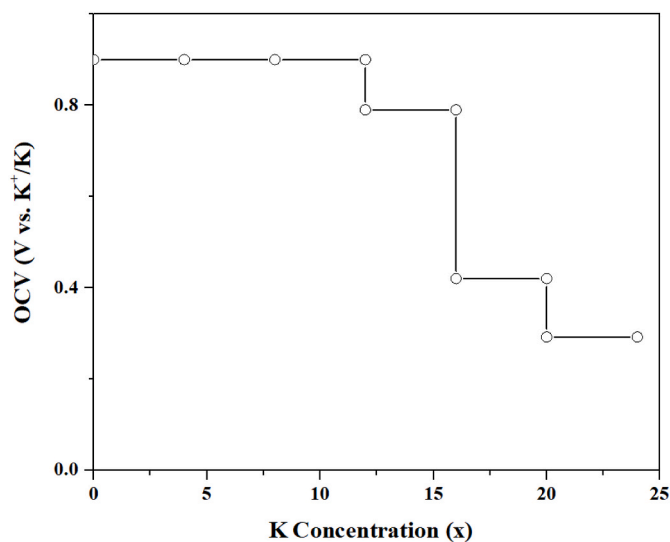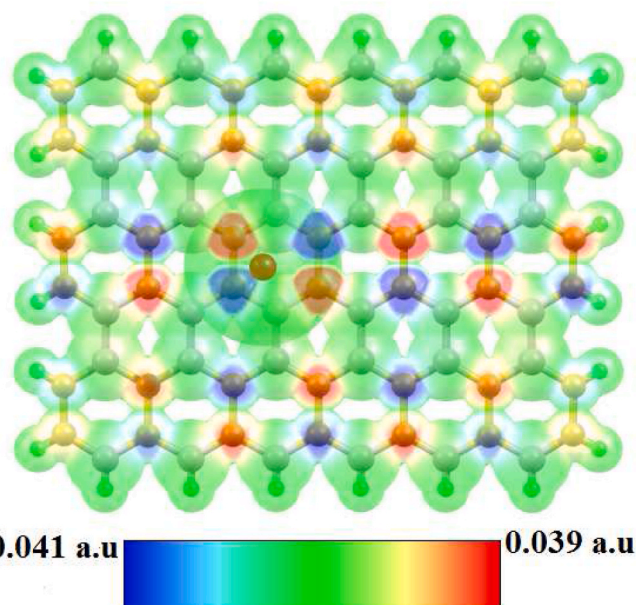

Fig. 4. Side vision of difference charge density ($\Delta\rho$) for adsorbed K-atom at the most stable binding site (H1) on o-B_2N_2 surface.

iso-surface distributed charge density diagrams. It can be seen that charge depletion shown by light-blue surrounds K atom, which shows that K atom contributes charge donation to the o-B_2N_2 monolayer, as a result, the electronegativities of the B and N atoms are higher compared to the potassium atom. In addition, the charge storage regions marked in yellow are located on the o-B_2N_2 surface and within the K atoms. Additionally, the CT method was performed using the Bader loading algorithm and the results are shown in Table 1. It is worth noting that each K has an electronic charge of about 0.889 |e|, lose on average.

In anode materials, the diffusion of K ions is another important factor that greatly affects the electrochemical performance of KIB, especially in the charge/discharge process. Therefore, it is employed to additional investigate of rate performance of o-B_2N_2 [48]. Therefore, the diffusion path of dilute K ions was evaluated by the minimum energy profile (MEP) using the NEB method. In the present study, the up sites of fully optimized scattering paths (A, B and C) were studied and their relative energy profiles are shown in Fig. 5. A typical path considered involves the migration of K ions along the a-direction (zigzag). Directions A and B (chair) are associated with pathways B and C on the H2 site of the o-B_2N_2 monolayer. In path A, we find that the K ions diffuse along chairs perpendicular to the boron-boron and nitrogen-nitrogen bonds, with a calculated minimum E_b of about 0.14 eV. On the other hand, in pathway B, the K ion diffuses from the more stable site (H1) along the a-direction parallel to the boron-boron and the nitrogen-nitrogen bond binds to the nearest H1. It is worth noting that the K ion must dominate E_b of 0.29 eV. In addition, pathway C indicates that K ion scatter over H2 with a calculated 0.33 eV MEP. Anticipated values of energy barrier match with binding energy values in Table 1, and diffusion barrier of K ion in path A deliver lowest energy profile among all paths. According to results, o-B_2N_2 monolayer can hopefully introduced as anode in new generation of batteries.

4. Conclusion

In summary, for the first time promising electrochemical attributes of two-dimensional o-B_2N_2 as a flexible anode for KIBs were investigated via various affecting agents based on DFT computations. Ionic-mobility, kinetics, and binding strength of K intercalation have been completely assessed. With a binding strength of −0.478 eV, K atoms are found to be
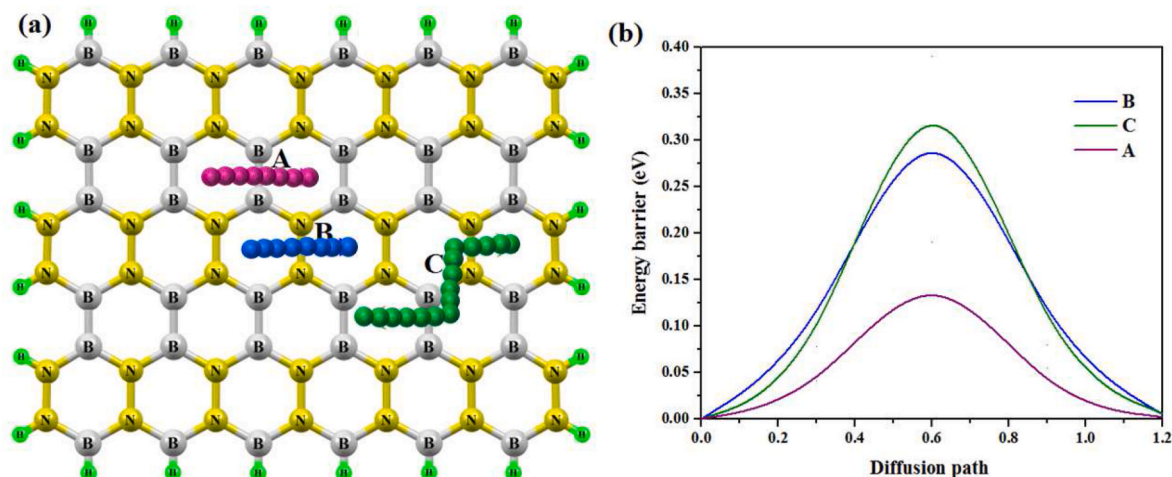

Fig. 3. Voltage profiles (V) with mean binding strength (eV) as a function of K concentration (x).

Fig. 5. (a) Upside vision of full optimized 3 different K-ion diffusion paths (A, B, and C). (b) Minimum energy barriers for K-ion along all paths.

stably inserted in B_2N_2 surface with no clustering and to preferentially have adsorption at hollow site of B_2N_2. In both sides of o-B_2N_2 surface, high K storage capacity can achieve a high value pf approximately 2347 mAh g^{-1} for theoretical specific capacity, which is remarkably higher in comparison to other 2D-materials for K-storage. In addition, a considerable benefit in high-performance KIBs was supplied by relatively low OCV of about 0.292 eV. According to mentioned outstanding electrochemical attributes, it can be anticipated that two-dimensional o-B_2N_2 delivers a promising potential to be employed as a novel battery electrode for KIBs. We therefore have a belief and hope that this work will serve as a guide for experimental and computational discussions on two-dimensional electrode materials.

Credit author statement

A.A. Rajhi, E. Hernández, C. Serrano, S.K. Saraswat: Conceptualization, Methodology, Software, Data curation, Writing-Original draft preparation. A.M. Mahmmod, H. sharif: Visualization, Investigation, Methodology, Reviewing and Editing. Y. A. Abdulsayed, A. Alawadi: Software, Validation, Data curation, Writing- Reviewing and Editing.

Declaration of competing interest

The authors declare that they have no known competing financial interests or personal relationships that could have appeared to influence the work reported in this paper.

Data availability

No data was used for the research described in the article.

Acknowledgments

The authors extend their appreciation to the Deanship of Scientific Research at King Khalid University, Saudi Arabia for funding this work through the Research Group Program under Grant No. RGP. 2/282/44.

Appendix A. Supplementary data

Supplementary data to this article can be found online at https://doi.org/10.1016/j.physb.2023.415324.

References

[1] C. Tang, M. Zhang, K. Zhang, J. Gong, Promising anode material BN/VS2 heterostructure for the Li-ion battery: the first-principles study, Appl. Surf. Sci. 564 (2021), 150468.
[2] X. Zhao, P. Wang, E. Lv, C. Wu, K. Ma, Z. Gao, I.D. Gates, W. Yang, Screening MXenes for novel anode material of lithium-ion batteries with high capacity and stability: a DFT calculation, Appl. Surf. Sci. 569 (2021), 151050.
[3] Q. Liao, S. Li, F. Xi, Z. Tong, X. Chen, X. Wan, W. Ma, R. Deng, High-performance silicon carbon anodes based on value-added recycling strategy of end-of-life photovoltaic modules, Energy 281 (2023), 128345.
[4] N. Khossossi, A. Banerjee, I. Essaoudi, A. Ainane, P. Jena, R. Ahuja, Thermodynamics and kinetics of 2D g-GeC monolayer as an anode materials for Li/Na-ion batteries, J. Power Sources 485 (2021), 229318.
[5] X. Zhang, W. Meng, T. He, L. Jin, X. Dai, G. Liu, Mn2C monolayer: a superior anode material offering good conductivity, high storage capacity and ultrafast ion diffusion for Li-ion and Na-ion batteries, Appl. Surf. Sci. 503 (2020), 144091.
[6] I. Muhammad, A. Ali, L. Zhou, W. Zhang, P.K.J. Wong, Vacancy-engineered half-metallicity and magnetic anisotropy in CrSI semiconductor monolayer, J. Alloys Compd. 909 (2022), 164797.
[7] R. Ren, F. Lai, X. Lang, L. Li, C. Yao, K. Cai, Efficient sulfur host based on Sn doping to construct Fe2O3 nanospheres with high active interface structure for lithium-sulfur batteries, Appl. Surf. Sci. 613 (2023), 156003.
[8] J. Wu, J. Yu, J. Liu, J. Cui, S. Yao, M.I.-U. Haq, N. Mubarak, A. Susca, F. Ciucci, J.-K. Kim, MoSe2 nanosheets embedded in nitrogen/phosphorus co-doped carbon/graphene composite anodes for ultrafast sodium storage, J. Power Sources 476 (2020), 228660.
[9] S.-F. Wang, B.-T. Wang, T. Bo, J.-R. Zhang, F.-W. Wang, Theoretical investigation of Ti2B monolayer as powerful anode material for Li/Na batteries with high storage capacity, Appl. Surf. Sci. 538 (2021), 148048.
[10] C. Yang, X. Sun, X. Zhang, J. Li, J. Ma, Y. Li, L. Xu, S. Liu, J. Yang, S. Fang, Is graphite nanomesh a promising anode for the Na/K-Ions batteries? Carbon 176 (2021) 242–252.
[11] L. Li, S. Jia, M. Cao, Y. Ji, H. Qiu, D. Zhang, Research progress on transition metal sulfide-based materials as cathode materials for zinc-ion batteries, J. Energy Storage 67 (2023), 107614.
[12] C. Zhu, S. Lin, M. Zhang, Q. Li, Z. Su, Z. Chen, Ultrahigh capacity 2D anode materials for lithium/sodium-ion batteries: an entirely planar B7P2 monolayer with suitable pore size and distribution, J. Mater. Chem. A 8 (2020) 10301–10309.
[13] S. Jana, S. Thomas, C.H. Lee, B. Jun, S.U. Lee, Rational design of a PC3 monolayer: a high-capacity, rapidly charging anode material for sodium-ion batteries, Carbon 157 (2020) 420–426.
[14] P. Xiang, X. Chen, B. Xiao, Z.M. Wang, Highly flexible hydrogen boride monolayers as potassium-ion battery anodes for wearable electronics, ACS Appl. Mater. Interfaces 11 (2019) 8115–8125.
[15] P. Xiang, S. Sharma, Z.M. Wang, J. Wu, U. Schwingenschlögl, Flexible C6BN monolayers as promising anode materials for high-performance K-ion batteries, ACS Appl. Mater. Interfaces 12 (2020) 30731–30739.
[16] X. Zhang, Y. Tang, F. Zhang, C.-S. Lee, A novel aluminum-graphite dual-ion battery, Adv. Energy Mater. 6 (2016), 1502588.
[17] M. Wang, C. Jiang, S. Zhang, X. Song, Y. Tang, H.-M. Cheng, Reversible calcium alloying enables a practical room-temperature rechargeable calcium-ion battery with a high discharge voltage, Nat. Chem. 10 (2018) 667–672.
[18] Y. Wu, W. Wei, T. Ding, S. Chen, R. Zhai, C. Bai, Modulating a 2D heterointerface with gC 3 N 4 mesh layers: a suitable hetero-layered architecture for high-power and long-life energy storage, J. Mater. Chem. A 9 (2021) 7791–7806.

[19] H. Șahin, S. Cahangirov, M. Topsakal, E. Bekaroglu, E. Akturk, R.T. Senger, S. Ciraci, Monolayer honeycomb structures of group-IV elements and III-V binary compounds: first-principles calculations, Phys. Rev. B 80 (2009), 155453.

[20] M. Topsakal, E. Aktürk, S. Ciraci, First-principles study of two-and one-dimensional honeycomb structures of boron nitride, Phys. Rev. B 79 (2009), 115442.

[21] Y. Hwang, Y.-C. Chung, Comparative study of metal atom adsorption on free-standing h-BN and h-BN/Ni (1 1 1) surfaces, Appl. Surf. Sci. 299 (2014) 29–34.

[22] Y. Hwang, Y.-C. Chung, Lithium adsorption on hexagonal boron nitride nanosheet using dispersion-corrected density functional theory calculations, Jpn. J. Appl. Phys. 52 (2013), 06GG08.

[23] S. Mu, Q. Liu, P. Kidkhunthod, X. Zhou, W. Wang, Y. Tang, Molecular grafting towards high-fraction active nanodots implanted in N-doped carbon for sodium dual-ion batteries, Natl. Sci. Rev. 8 (2020).

[24] D. Xie, M. Zhang, Q. Liu, Y. Lin, A. Yu, Y. Tang, Organic-inorganic conformal extending high-purity metal nanosheets for robust electrochemical lithium-ion storage, Adv. Funct. Mater. 2306291 (2023). https://doi.org/10.1002/adfm.202306291.

[25] S. Demirci, S.E. Rad, S. Kazak, S. Nezir, S. Jahangirov, Monolayer diboron dinitride: direct band-gap semiconductor with high absorption in the visible range, Phys. Rev. B 101 (2020), 125408.

[26] R.L. Kumawat, B. Pathak, Strong anisotropy and band Gap engineering with mechanical strains in two-dimensional orthorhombic diboron dinitride (O-B2N2), Appl. Surf. Sci. 586 (2022), 152850.

[27] R. Rahimi, M. Solimannejad, High-performance hydrogen storage properties of Li-decorated B2N2 nanosheets: a periodic density functional theory study, Energy Fuels 35 (2021) 6858–6867.

[28] W. Hao, J. Xie, Reducing diffusion-induced stress of bilayer electrode system by introducing pre-strain in lithium-ion battery, Journal of Electrochemical Energy Conversion and Storage 18 (2021), 020909.

[29] S. Grimme, Accurate description of van der Waals complexes by density functional theory including empirical corrections, J. Comput. Chem. 25 (2004) 1463–1473.

[30] K. Adhikari, A.K. Ray, Carbon- and silicon-capped silicon carbide nanotubes: an ab initio study, Phys Lett Sect A Gen At Solid State Phys 375 (2011) 1817–1823.

[31] A.A. Peyghan, M.B. Tabar, S. Yourdkhani, A theoretical study of OH and OCH3 free radical adsorption on a nanosized tube of BC2N, J. Cluster Sci. 24 (2013) 1–10.

[32] J. Du, X. Sun, G. Jiang, Structures, chemical bonding, magnetisms of small Al-doped zirconium clusters, Phys Lett Sect A Gen At Solid State Phys 374 (2010) 854–860.

[33] X. Liu, B. Zhu, Y. Gao, Structure stability of TiAu4 nanocluster with water adsorption, Phys Lett Sect A Gen At Solid State Phys 380 (2016) 1971–1975.

[34] S. Bashiri, E. Vessally, A. Bekhradnia, A. Hosseinian, L. Edjlali, Utility of extrinsic [60] fullerenes as work function type sensors for amphetamine drug detection: DFT studies, Vacuum 136 (2017) 156–162.

[35] M.W. Schmidt, K.K. Baldridge, J.A. Boatz, S.T. Elbert, M.S. Gordon, J.H. Jensen, S. Koseki, N. Matsunaga, K.A. Nguyen, S. Su, T.L. Windus, M. Dupuis, J. A. Montgomery Jr., General atomic and molecular electronic structure system, J. Comput. Chem. 14 (1993) 1347–1363.

[36] W. Tang, E. Sanville, G. Henkelman, A grid-based Bader analysis algorithm without lattice bias, J. Phys. Condens. Matter 21 (2009), 084204.

[37] G. Henkelman, B.P. Uberuaga, H. Jónsson, A climbing image nudged elastic band method for finding saddle points and minimum energy paths, The Journal of chemical physics 113 (2000) 9901–9904.

[38] J. Xie, X. Wei, X. Bo, P. Zhang, P. Chen, W. Hao, M. Yuan, State of charge estimation of lithium-ion battery based on extended Kalman filter algorithm, Front. Energy Res. 11 (2023), 1180881.

[39] Z. Zhao, T. Yu, S. Zhang, H. Xu, G. Yang, Y. Liu, Metallic P 3 C monolayer as anode for sodium-ion batteries, J. Mater. Chem. A 7 (2019) 405–411.

[40] S. Mukherjee, L. Kavalsky, C.V. Singh, Ultrahigh storage and fast diffusion of Na and K in blue phosphorene anodes, ACS Appl. Mater. Interfaces 10 (2018) 8630–8639.

[41] B. Byles, N. Palapati, A. Subramanian, E. Pomerantseva, The role of electronic and ionic conductivities in the rate performance of tunnel structured manganese oxides in Li-ion batteries, Apl. Mater. 4 (2016).

[42] C.R. Dean, A.F. Young, I. Meric, C. Lee, L. Wang, S. Sorgenfrei, K. Watanabe, T. Taniguchi, P. Kim, K.L. Shepard, Boron nitride substrates for high-quality graphene electronics, Nat. Nanotechnol. 5 (2010) 722–726.

[43] H.R. Jiang, W. Shyy, M. Liu, L. Wei, M.C. Wu, T.S. Zhao, Boron phosphide monolayer as a potential anode material for alkali metal-based batteries, J. Mater. Chem. A 5 (2017) 672–679.

[44] X. Zhang, L. Jin, X. Dai, G. Chen, G. Liu, Two-dimensional GaN: an excellent electrode material providing fast ion diffusion and high storage capacity for Li-ion and Na-ion batteries, ACS Appl. Mater. Interfaces 10 (2018) 38978–38984.

[45] D. Er, J. Li, M. Naguib, Y. Gogotsi, V.B. Shenoy, Ti3C2 MXene as a high capacity electrode material for metal (Li, Na, K, Ca) ion batteries, ACS Appl. Mater. Interfaces 6 (2014) 11173–11179.

[46] Q. Tang, Z. Zhou, P. Shen, Are MXenes promising anode materials for Li ion batteries? Computational studies on electronic properties and Li storage capability of Ti3C2 and Ti3C2X2 (X= F, OH) monolayer, J. Am. Chem. Soc. 134 (2012) 16909–16916.

[47] H. Lin, G. Liu, L. Zhu, Z. Zhang, R. Jin, Y. Huang, S. Gao, Flexible borophosphene monolayer: a potential Dirac anode for high-performance non-lithium ion batteries, Appl. Surf. Sci. 544 (2021), 148895.

[48] S.-Y. Chung, Y.-M. Chiang, Microscale measurements of the electrical conductivity of doped LiFePO4, Electrochem. Solid State Lett. 6 (2003) A278.